3 November 2000

ELSEVIER

Chemical Physics Letters 330 (2000) 68–76

CHEMICAL PHYSICS LETTERS

www.elsevier.nl/locate/cplett

Fourier transform infrared spectroscopic study of Br_2O and OBrO

Liang T. Chu [a,1], Zhuangjie Li [b,*]

[a] *Wadsworth Center and Department of Environmental Health and Toxicology, State University of New York, P.O. Box 509, Albany, NY 12201-0509, USA*

[b] *Department of Atmospheric Sciences, University of Illinois at Urbana-Champaign, Urbana, IL 61801, USA*

Received 1 June 2000; in final form 30 August 2000

Abstract

Vibrational frequencies of gaseous Br_2O and OBrO were observed using the Fourier transform infrared spectrometer. For the first time, bands at 629.0 cm^{-1} (ν_3) and 532.9 cm^{-1} (ν_1) were recorded for both Br–O asymmetric and symmetric stretching vibrations of gaseous Br_2O. Two fundamental vibrations were observed at 798.7 cm^{-1} (ν_1) and 846.3 cm^{-1} (ν_3) for the $O^{18}BrO$ radical. In addition, two new peaks at 2333 cm^{-1} and 668 cm^{-1} were observed in a HOBr spectrum. They are tentatively assigned to the H–Br and Br–O stretching vibrations of a HOBr isomer on the basis of ab initio computational results.

1. Introduction

Characterization of halogen-containing species is important for improving the current understanding of atmospheric halogen chemistry leading to stratospheric ozone depletion. Chlorine- and bromine-containing species have been the focus of many investigations, since they play a vital role in causing both the ozone decline on a global scale in last three decades and the Antarctic ozone hole during the Antarctic spring since the late 1970s [1]. However, the chlorine- and bromine-containing species and their chemistry are not equally well understood. Many chlorine-containing species involved in atmospheric and laboratory studies, such as OClO, HOCl, and Cl_2O, have been extensively characterized and documented [2], but their analogous brominated species received much less examination. This is partially due to the fact that atmospheric bromine is much less abundant than chlorine [1]. In addition, atmospheric bromine chemistry is quite complex, and hence has not been explored in detail [3,4]. Recent findings of a higher efficiency of catalytic removal of ozone by bromine than chlorine on a per atom basis in the polar stratosphere invites a thorough investigation of the bromine chemistry [1,5], which in turn requires characterization of each brominated species. Among the inorganic bromine species are OBrO, a species recently detected in the mid-latitude stratosphere [6,7], HOBr, a product from the reaction of BrO with HO_2 and the hydrolysis of $BrONO_2$ [8,9], and Br_2O, a precursor of HOBr in laboratory studies [10]. They are the analogues of OClO, HOCl, and Cl_2O, respectively.

* Corresponding author. Fax: +1-217-244-4393.

E-mail addresses: lchu@csc.albany.edu (L.T. Chu), zli@atmos.uiuc.edu (Z. Li).

[1] Also corresponding author. Fax: +1-518-473-2895.

0009-2614/00/$ - see front matter
PII: S0009-2614(00)01090-3

Fourier transform infrared (FTIR) spectroscopic study of gas-phase bromine-containing species can provide important information regarding the fundamental vibrations of the molecules examined. However, the study may also be a challenging task since the vibrations associated with bromine atoms fall into a lower frequency domain and have a narrower rotational energy spacing. Furthermore, the bromine atom is in general weakly bonded to other atoms in inorganic brominated molecules or radicals. The weak bonds between bromine and other atom(s) often result in unstable brominated species, which make the detection and detailed study of brominated species more difficult than their chlorine analogs. For these reasons, reports on the infrared study of the brominated radicals and compounds are sparse. In the case of OBrO, FTIR spectra of OBrO in an argon or nitrogen matrix have been determined by Kölm et al. [11] and Tevault et al. [12]. Miller et al. [13,14] have recently reported a value of 848.6 cm^{-1} for the ν_3 Br–O stretching vibration on the basis of the first gas-phase OBrO FTIR spectrum in the region of 810–880 cm^{-1}. They also determined the frequencies of both ν_1 and ν_2 bands by analyzing the electronic absorption spectrum of the OBrO radical. The IR spectrum of Br_2O and BrBrO in solid argon matrices was first studied by Tevault et al. [12] and recently by Kölm et al. [15]. Müller and Cohen [16] have examined the microwave Br_2O spectrum. Very little information is available in the literature regarding the infrared investigation of the gas-phase Br_2O molecule.

The OBrO radical has recently been synthesized and collected in quantity at low temperature [17]. One goal of this study was to demonstrate that this is also a good OBrO source for spectroscopic studies. The gaseous Br_2O FTIR spectrum was not reported in the literature. The FTIR spectra are useful to atmospheric chemists investigating BrO_x chemistry via IR detection schemes. It is also a starting point for conducting the high-resolution IR spectra for gas-phase Br_2O and OBrO. This motivated us to record the IR spectra of these species. In this paper, we report an infrared spectroscopic study of gaseous Br_2O and OBrO in the range of 4000–500 cm^{-1}. An IR spectrum of HOBr, which was produced by the hydrolysis of Br_2O, is briefly investigated. As discussed later, a new species was observed in the FTIR spectra along with HOBr, which is ascribed to an isomer of HOBr.

2. Experimental

The gas-phase infrared spectra were taken on a Mattson RS-2 FTIR spectrometer. The major components of the experimental apparatus used in the present work are illustrated in Fig. 1. The spectrometer was equipped with a KBr beam splitter and a liquid nitrogen cooled HgCdTe (MCT) detector. Its sample compartment housed a 3.2 m (total pathlength) multipass absorption cell (Wilmad Glass) with aluminum mirrors and either NaCl or KBr windows. The multipass-cell could be continually evacuated by pumping to reduce the loss of short-lived species such as OBrO. The IR absorption cell was cooled to 250 K using dried cooled nitrogen gas when the IR spectrum of the OBrO radical was taken. Both Teflon tubing and glass tubing were used to transfer the OBrO radicals into the cell. The spectra were recorded at 0.5 cm^{-1} resolution with 32–64 co-added scans.

The OBrO radicals were generated by flowing a mixture of $\sim 10^{13}$ molecules/cm^3 of Br_2 (Aldrich) and $\sim 10^{14}$ molecules/cm^3 ultra-high purity oxygen (Praxair), carried by 1000 sccm of ultra-high purity helium (Praxair), through a 2.45 GHz microwave discharge (Opthos Instruments, MPG-4M) cavity [17]. The gas flow rates were controlled by stainless steel mass flow controllers (Teledyne-Hastings). The pressure in the microwave discharge zone was maintained at approximately 1 Torr by a large mechanical pump (Alcatel 2063C). Bromine was purified by a pump-and-thaw procedure before being mixed with helium. The microwave discharge power was adjusted in the range of 30–40 W. Products from the microwave discharge of the Br_2/O_2/He mixture were trapped in a U-tube at $\sim$240 K. The OBrO sample was collected for $\sim$1 h before it was warmed to 273 K and then transferred to the absorption cell with helium carrying gas through a short transfer tube (10–15 cm). The total pressure in the IR cell was maintained at approximately 25 Torr during the recording of the

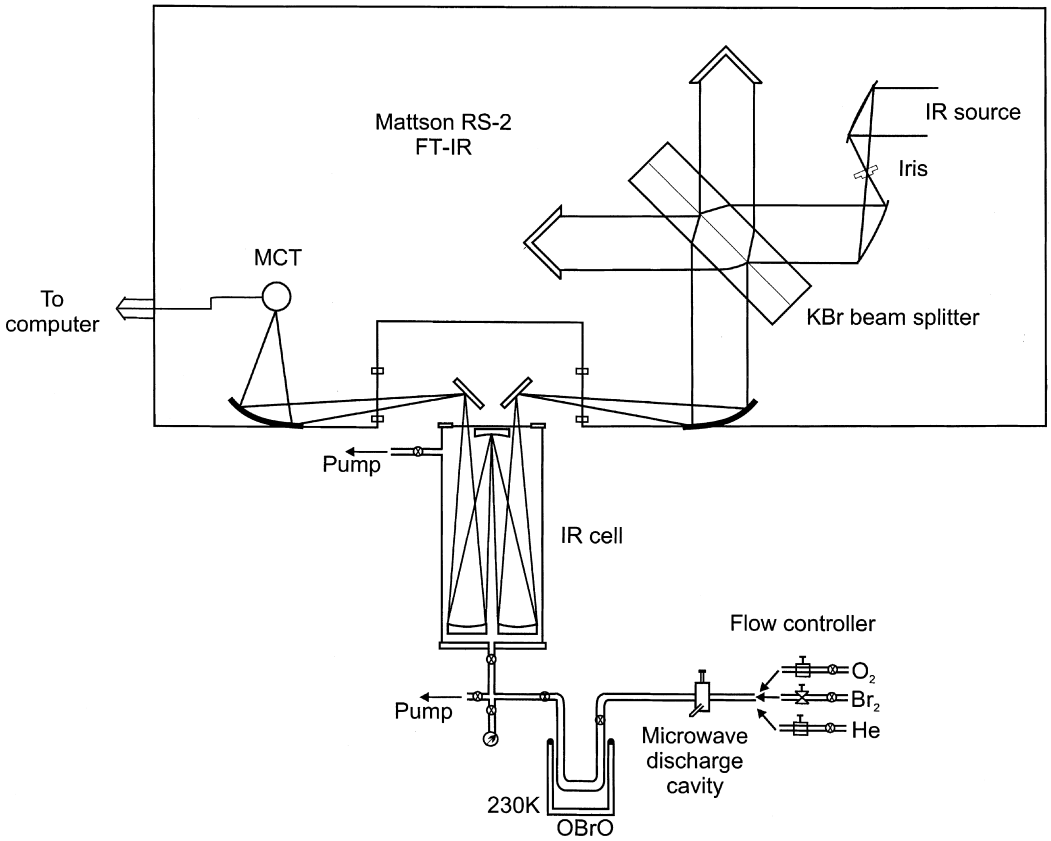

Fig. 1. Schematic diagram of the experimental apparatus for FTIR studies of OBrO and Br_2O.

OBrO IR spectrum and the OBrO residence time in the cell was approximately 20 ms. In a separate experiment, the synthesized OBrO radicals were also detected by a quadrupole mass spectrometer at its parent ion $m/e = 111, 113$, which corresponds to $O^{79}BrO^+$ and $O^{81}BrO^+$, respectively.

The Br_2O molecules were synthesized by the heterogeneous reaction of the bromine vapor with HgO [10,15]:

$$2Br_2 + HgO(s) \rightarrow HgBr_2(s) + BrOBr \quad (1)$$

50–100 g of HgO (yellow) powder (Aldrich) were mixed in glass wool and placed in a glass flask equipped with both inlet and outlet valves. The flask was evacuated to 10^{-3} Torr and heated to approximately 370 K for about one hour prior to its use for reaction (1). Bromine was first frozen to degas and then dried by passing through a P_2O_5 (Aldrich) trap to remove the moisture. The evacuated flask was then filled with dried bromine up to ~100 Torr at 273 K in the dark. After allowing approximately 5 min of mixing and reaction for reactants and products, gases were transferred into a liquid nitrogen cooled trap. This procedure was repeated about 10 times to obtain a sufficient quantity of Br_2O. The sample trap was then pumped at 245 K to remove the Br_2 impurity in the Br_2O sample. The trap was kept at 245 K to avoid Br_2O decomposition at 255 K as suggested in the literature [18]. A green-brownish Br_2O powder then remained in the trap. The multipass IR absorption cell was evacuated to 10^{-3} Torr and gas-phase Br_2O was transferred into the cell at 273 K. The cell was then sealed. IR spectra were taken at a total pressure of approximately 1 Torr.

3. Results

3.1. OBrO FTIR spectrum

When OBrO was continuously flowed through the absorption cell at a total pressure of 25 Torr, the FTIR spectrum was recorded with a resolution of 0.5 cm^{-1} at 250 K using NaCl windows and a narrow-band MCT detector. The spectrum was scanned from 700–4000 cm^{-1}. A typical IR spectrum of OBrO is shown in Fig. 2. Two absorption bands were observed in the 790–860 cm^{-1} region as shown in Fig. 2. The isotope effect of the ν_3 band (Br–O asymmetric stretching) was observed as two peaks separated by about 2.2 cm^{-1}, at 848.5 and 846.3 cm^{-1}. A pair at 800.4 and 798.7 cm^{-1} was also observed for the ν_1 band (Br–O symmetric stretching) for the ^{79}Br and ^{81}Br isotope effects in the OBrO radical, respectively. The cut-off frequency of the narrow-band MCT detector was about 750 cm^{-1}. Below the cut-off frequency, a high level of noise appeared in the spectrum. The ν_2 vibrational mode (O–Br–O bending) was at an even lower frequency region and was not observed with this apparatus. The results of our FTIR spectrum analysis on the gaseous OBrO radical are summarized in Table 1 along with the available IR data for this radical.

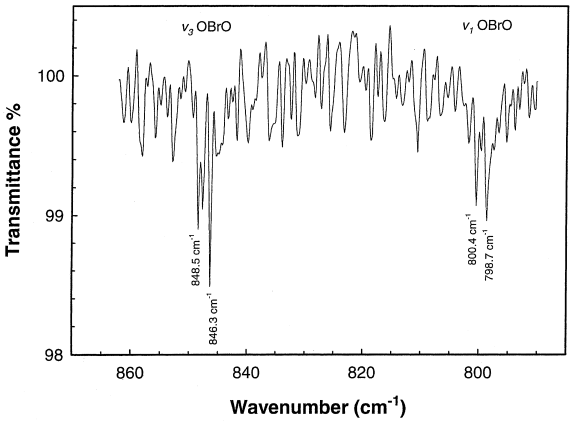

Fig. 2. OBrO FTIR spectrum. The spectrum was recorded at a resolution of 0.5 cm^{-1} with 32 scans at 250 K. NaCl windows were used. The OBrO radicals were carried by helium into the IR cell. The total pressure in the cell was about 25 Torr.

3.2. Br_2O FTIR spectrum

The Br_2O IR spectra consisted of 64 co-added scans at 0.5 cm^{-1} resolution, after Br_2O was introduced into the static IR cell equipped with KBr windows. A wide-band MCT detector was used to record these spectra. Absorption peaks at 532 and 629 cm^{-1} due to Br_2O molecules were observed as shown in Fig. 3. These peaks disappeared quickly

Table 1
Observed IR frequencies (in cm^{-1}) of OBrO

Isomers	Modes	This work (gas-phase)	Calculated	Miller et al. [13] (gas-phase)	Kölm et al. [11] (Ar matrix)	Tevault et al. [12] (N_2 matrix)	Maier and Bothur [26] (Ar matrix)
$^{16}O^{79}Br^{16}O$	ν_1	800.4 ± 1.0		799.4[c]	795.7		
$^{16}O^{79}Br^{16}O$	ν_3	848.5 ± 1.0 (1.1 ± 0.4)[a]	848.5[b]	848.6	845.2	851.9	846.6
$^{16}O^{81}Br^{16}O$	ν_1	798.7 ± 1.0		799.4[c]	794.6		
$^{16}O^{81}Br^{16}O$	ν_3	846.3 ± 1.0 (1.4 ± 0.6)[a]	846.2	846.3	842.8	849.6	844.7, 842.8
$^{18}O^{79}Br^{18}O$	ν_1				756.4		
$^{18}O^{79}Br^{18}O$	ν_3		811.0		808.4	813.9	
$^{18}O^{81}Br^{18}O$	ν_1				806.1	811.6	
$^{18}O^{81}Br^{18}O$	ν_3		808.6		755.0		
$^{18}O^{79}Br^{16}O$	ν_3					839.9	

[a] The number in the parenthesis is the absorbance intensity ratio of ν_3/ν_1. The large error bar takes the noisy background into consideration.
[b] The calculation was based on this frequency.
[c] Determined from spectral fitting (see text for details).

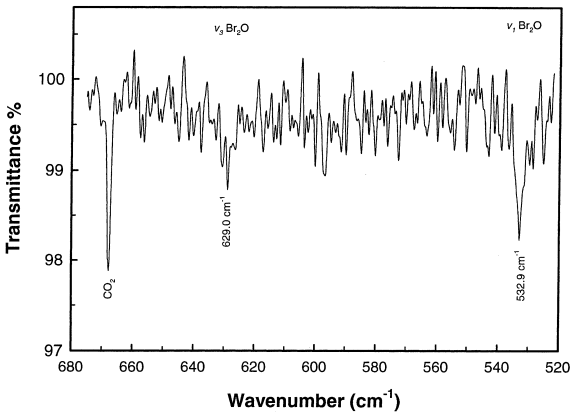

Fig. 3. Br_2O FTIR spectrum at 298 K. The spectrum was collected with 64 co-added scans at 0.5 cm^{-1}resolution. The Br_2O pressure in the cell was about 1 Torr. A background level CO_2 is included in the spectrum to illustrate the signal level.

after ~10 min suggesting that Br_2O was not very stable in the IR cell. We assigned these vibrational transitions to the symmetric Br–O stretching (ν_1) and the asymmetric Br–O stretching (ν_3) vibration of the Br_2O molecule on the basis of ab initio frequency calculations for the Br_2O molecule [19]. These frequencies are in good agreement with those observed in the Br_2O Ar/N_2 matrix IR spectra, after taking into consideration the red-shift in frequency (a factor of 1.014 for Ar matrix [20]) [15,21,22]. To the best of our knowledge, there is no gas-phase IR spectrum reported in this frequency region for the Br_2O molecule. The isotope effect (^{79}Br versus ^{81}Br) on the vibrational frequencies was not observed in our Br_2O infrared spectra in the present study, indicating that they are not resolved under the current resolution conditions. This will be discussed later.

With the presence of water vapor in the Br_2O sample (HgO and/or U-tube), the Br_2O molecule was found to be hydrolyzed rapidly. During experiments, we noticed that if there was water vapor (best estimated to be <0.1 Torr) in the IR cell, a few new absorption peaks appeared in the spectrum. Meanwhile, absorption peaks of the Br_2O molecule were below the detection limit. Fig. 4a shows a typical spectrum of this observation. Two pronounced peaks centered at 3614.5 cm^{-1} (ν_1) and 1163.1 cm^{-1} (ν_2), along with a relatively weaker peak at 620.8 cm^{-1} (ν_3), are ascribed to the HOBr molecule. The relative absorption intensity ratio for the peaks is 4.6:2.8:1 for ν_1, ν_2, and ν_3, respectively. The absorption intensity of the three vibrational bands for HOBr molecules was decreased nearly to the noise level in 20–30 min; this was probably due to a combination of photo- and thermal decomposition of the HOBr molecule in the IR cell.

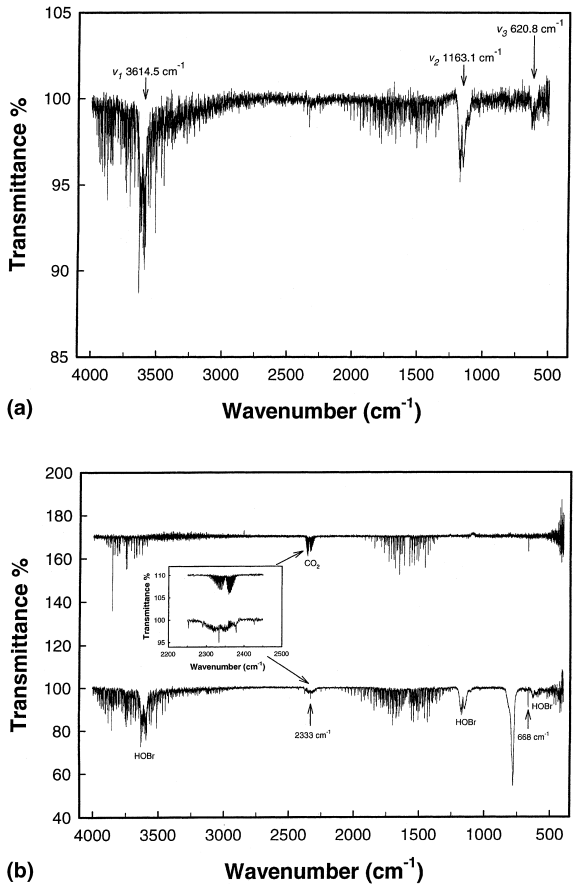

Fig. 4. a. A typical HOBr FTIR spectrum obtained by the hydrolysis of Br_2O in the reaction flask containing a trace amount of water. The vibrational bands are indicated by arrows. KBr windows were used to record this spectrum. The HOBr absorption peaks disappeared in ~30 min and a peak at 789 cm^{-1} grew rapidly. b. Two peaks at 2333 and 668 cm^{-1} coexisted with the HOBr absorption peaks. The FTIR spectrum of CO_2 and water is provided on top of the HOBr spectrum for comparison. The inserted figure shows detailed features of the 2333 cm^{-1} band.

In all the IR spectra taken, we observed, more or less, three other bands in addition to the bands due to both HOBr and H_2O molecules. The bands were centered at 2333, 668 and 789 cm^{-1}, respectively (see Fig. 4b). We noticed that the initial peak intensity at 789 cm^{-1} was substantially lower than that at 1163.1 cm^{-1} (see Fig. 4a). The 789 cm^{-1} peak was found to grow rapidly with time as the HOBr absorption intensity decreased, suggesting that the peak may possibly come from HOBr decomposition products. However, we could not positively identify whether this peak was due to a gas-phase species, or due to some species adsorbed on the windows/mirrors of the cell.

4. Discussion

4.1. OBrO spectrum assignment

The isotope effect on the OBrO radical provided a means to show the consistency of the spectrum assignment. The observed ν_3 band isotope frequency ratio was $\nu_3^{81}/\nu_3^{79} = 0.9974$. The isotope effect on the asymmetric frequency can be calculated on the basis of the Teller–Redlich product rule [23]

$$\frac{\nu_3^{81}}{\nu_3^{79}} = \left(\frac{m_{Br}\left(m_{Br}^{81} + 2m_O \sin^2\alpha\right)}{m_{Br}^{81}\left(m_{Br} + 2m_O \sin^2\alpha\right)}\right)^{1/2}, \quad (2)$$

where m_{Br} is the mass of the bromine atom, m_O the mass of the oxygen atom, and α is half the O–Br–O bond angle. Using $\alpha = 57.48°$ [13], the ratio ν_3^{81}/ν_3^{79} was calculated to be 0.9972. This value is in excellent agreement with the observed value. The asymmetric frequency of various OBrO isotopes under the central forces assumption was calculated and listed in Table 1. It can be seen from Table 1 that our measured frequency for the ν_3 vibration of the OBrO radical is in excellent agreement with that measured by Miller et al. [13]. Miller et al. also determined the ν_1 frequency of gaseous OBrO to be 799.4 cm^{-1} by a fit of observed vibrionic features in the OBrO $C(^2A_2) \leftarrow X(^2B_1)$ absorption spectrum. With a difference of $\leqslant 1$ cm^{-1}, our measured frequency at 798.7 or 800.4 cm^{-1} for the ν_1 mode of gaseous OBrO is in good agreement with their value. Table 1 also lists the IR OBrO matrix data for comparison. The vibrational frequency appears to be higher in the gas-phase than in the argon matrix for the OBrO radical. This reflects the fact that radicals in the gaseous phase experience far fewer and weaker inter-molecular interactions than in the solid-phase, and interactions in the solid-phase could probably account for the red-shift in the frequency of OBrO vibrational motions. We assume that the frequency shift from the gas-phase to the Ar matrix for OBrO is similar to that of OClO, which was determined to be $\nu^{gas}/\nu^{Ar} = 1.0028$ and 1.00488 for the ν_3 and ν_1 modes, respectively [24,25]. Under this approximation, our assignments are in very good agreement with the assignments of both Kölm et al. [11] and Maier and Bothur [26].

4.2. Br_2O spectrum analysis

Although relatively strong adsorption peaks at 532.9 and 629.0 cm^{-1} were observed in the Br_2O FTIR spectrum (see Fig. 3), we were unable to resolve the ^{79}Br or ^{81}Br isotope effects of these vibrations. This can be justified on the basis of the product rule. The frequency ν_3 ratio can be calculated from

$$\frac{\nu_3^{81}}{\nu_3^{79}} = \left(\frac{m_{Br}(m_O + 2m_{Br}^{81}\sin^2\alpha)}{m_{Br}^{81}(m_O + 2m_{Br} + \sin^2\alpha)}\right)^{1/2} \quad (3)$$

to be 0.9984 using $\alpha = 56.1°$ [19]. The frequency separation is approximately $^{79}\nu_3 - {}^{81}\nu_3 = 0.9$ cm^{-1}. Clearly, the two bands overlapped and were unlikely to be well resolved with our instrument.

Table 2 compares our IR measurements with the previous IR matrix data for the Br_2O molecule. It can be seen from Table 2 that the two observed Br–O frequencies agree well with those observed in an argon matrix at 17 K, after the stretching frequencies are scaled by 1.014 from the argon matrix data, i.e., 525.3 and 622.2 cm^{-1}, to the gas-phase data [20].

In addition to the absorption peaks positively assigned to HOBr in Fig. 4a, there are two absorption peaks at 2333 and 668 cm^{-1} in the FTIR spectrum (see Fig. 4b), which do not seem to belong to HOBr. These peaks partially overlap with

Table 2
The observed IR frequencies (in cm^{-1}) of Br_2O

Modes	This work (gas-phase)	Kölm et al. [15] (Ar matrix)	Tervault et al. [12] (Ar matrix)	Allen et al. [22] (Ar matrix)	Levason et al. [21] (N_2 matrix)
ν_1	532.9 ± 1.0 (1.7 ± 0.6)[a]	525.3	526.1	526.1	528
ν_3	629.0 ± 1.0	622.2		623.4	626

[a] The number in the parenthesis is the absorbance intensity ratio of ν_1/ν_3.

the CO_2 absorption peaks at 2349.3 and 667.3 cm^{-1} [23], but as shown in the top panel of Fig. 4b, the line shape and intensity patterns of these peaks are clearly different from those of CO_2 (see inserted figure). Therefore the peaks are not due to CO_2. Since there were only three elements in the sample, namely H, O, and Br, the only species constructed from these three elements could give rise to these two peaks. Indeed, these peaks seem to have absorption features associated with stretching and bending vibrations for compounds made up of these elements. One evidence is that the 2333 cm^{-1} band resembles the H–Br stretching mode. However, this band cannot be gas-phase HBr since the HBr vibrational absorption is at 2559.3 cm^{-1} [27]. One possible species that could contribute to these new IR absorption peaks is an isomer of HOBr, i.e., HBrO, in which the bromine atom is bonded to both hydrogen and oxygen atoms. The vibrational frequencies of HBrO were predicted to be 2292, 818, and 665 cm^{-1} at the CCSD(T)/TZ2P level of theory, and 2360, 837, and 705 cm^{-1} at the CCSD(T)/6-311++G(3df,3pd) level of theory for H–Br stretching (ν_1), H–Br–O bending (ν_2), and Br–O stretching vibrations (ν_3), respectively [19]. The IR absorption intensity of the ν_2 band was also predicted to be 22- and 40-fold weaker than that of the ν_1 and ν_3 bands, respectively [19]. This suggests that the vibration mode at 818 cm^{-1} is unlikely to be observed. Thus within an uncertainty of less than 6%, the vibrational peaks observed at 2333 and 668 cm^{-1} match the theoretical predictions for the HBrO molecule. On the basis of the above argument, we may *tentatively* assign the observed peaks at 2333 and 668 cm^{-1} to the H–Br stretching and Br–O stretching modes of the HBrO molecule.

There could be a possibility that both 2333 and 668 cm^{-1} bands were from other $HBrO_x$ ($x = 2$–4) compounds. However, it is unlikely that these bands arise from HOBrO, $HOBrO_2$ and $HOBrO_3$. This is simply due to the fact that hydrogen in these molecules does not directly bond to bromine and thus there is no H–Br stretching mode for these compounds. An isomer of HOBrO and $HOBrO_2$ has a structure of $HBrO_2$ and $HBrO_3$, respectively, which has a H–Br stretching vibration. The H–Br stretching frequency was calculated to be at 1915 and 2154 cm^{-1} for $HBrO_2$ and $HBrO_3$, respectively [29,30]. These frequencies are substantially lower than the H–Br stretching frequency observed in our spectrum. It was also noticed that $HBrO_2$ was predicted to have a few transitions at 794, 868, and 898 cm^{-1} [29]. Among them, the band at 868 cm^{-1} is the strongest one. $HBrO_3$ was predicted to have a stronger BrO asymmetric stretching mode at 966 cm^{-1} than the H–Br stretching vibration [30]. But neither of these frequencies matches with our observations. We may thus exclude both $HBrO_2$ and $HBrO_3$ isomers in contributing to the observed spectrum in the present study. It remains that HBrO is the most likely molecule observed in our experiment.

There are questions remaining in the assignment of these two peaks to the HBrO molecule. It is unclear how HBrO was formed in the present study. Li and Franciso [28] suggested that HBrO is unlikely to be formed in the gas-phase by the reaction of Br_2O with H_2O. Because HOBr is 57 kcal mol^{-1} more stable than HBrO, the formation of HBrO from the reaction of Br_2O with H_2O ($\Delta H = 116$ kcal mol^{-1}) is thermodynamically unlikely. Also, there is an activation energy barrier of 75 kcal mol^{-1} for the HOBr isomerization to HBrO [28]. Thus, it is unfavorable to convert HOBr into HBrO in the gas-phase. However, HBrO molecules might be heterogeneously produced and this is discussed as follows.

Br_2O was synthesized by heterogeneous reaction (1). If there is a trace amount of water vapor in the reactor, one may expect that adsorbed bromine may react with the adsorbed water to form HBrO on HgO. The process is illustrated as follows:

$$H_2O(ad) + Br\text{–}OHg(ad) \rightarrow \text{intermediates}(ad) \rightarrow HBrO(ad) + \text{other products.} \quad (4)$$

The notation (ad) in the above chemical equation represents the adsorbed species. This process could also form HOBr(ad), but we will focus only on the HBrO channel here. It is important to point out that this scheme is different from the unfavorable gas-phase conversion discussed previously. Adsorption on the HgO surface will lead to changes in the thermodynamic properties of both reactants and products. For example, the heat of adsorption for H_2O on many metal surfaces is $\Delta H_{ad}(H_2O) = 12$ kcal mol^{-1} [31]. The entropy change is expected to be small since all species are adsorbed on the surface and, for simplicity, we may use enthalpy to discuss the reaction. We will adapt this value for the adsorption of H_2O on HgO surfaces. The heat of adsorption of Br_2 on mercury surfaces can be estimated from an empirical correlation [32], it is about -5 kcal mol^{-1}. Since we adapted $\Delta H_{ad}(H_2O) = -12$ kcal mol^{-1} on metal surfaces, we will employ the same treatment for Br_2, i.e., $\Delta H_{ad}(Br_2) = -5$ kcal mol^{-1}. The overall reaction enthalpy for reaction (4), ΔH_r, is then mainly controlled by H_2O(ad) and HBrO(ad). Assuming the heat of adsorption for HBrO is similar to that of HOBr ($\Delta H = -16$ kcal mol^{-1}) [33], one would expect that ΔH_r for reaction (4) is close to zero ($\Delta H_r = \Delta H_{ad}(HBrO) - \Delta H_{ad}(Br_2) - \Delta H_{ad}(H_2O) = 1$ kcal mol^{-1}). Taking the uncertainty of calculations into consideration; it is therefore reasonable to say that reaction (4) could take place on the HgO surface. The product HBrO(ad) is expected to desorb to the gas-phase as observed by our FTIR spectrometer. However, this proposed scenario is subject to experimental examination that could not be carried out with the current apparatus, and additional studies are required to confirm the assignment of these new peaks for the HBrO molecule and the HBrO formation mechanism.

5. Summary

Gas-phase IR spectra of inorganic bromine species OBrO and Br_2O were collected using a multipass cell in the FTIR apparatus. The effect of the isotope on the vibrational spectrum for OBrO was determined and calculated. The gas-phase Br_2O FTIR spectrum in the mid-infrared region is reported for the first time. With the presence of water vapor, Br_2O was found to hydrolyze into HOBr. Two new absorption features were observed along with the HOBr spectrum, and they are tentatively assigned to the isomer of HOBr.

Acknowledgements

The authors would like to thank Professor Arthur Fontijn and Professor Steven Bernasek for kindly lending the microwave generator and the wide-band MCT detector, respectively, to be used in the FTIR system for this work at the Wadsworth Center. Discussion with Dr. Oliver Rattigan and Professor Charles Miller during the course of this study was appreciated. This work was supported by the National Science Foundation ATM-9530659 and ATM-9813331, and by the EPA research grant (X825967-01-0 EPA).

References

[1] WMO, Scientific assessment of ozone depletion: 1994, WMO Global Ozone Research and Monitoring Project-Report No. 37, WMO, Geneva, 1995, and references within.
[2] W.B. Demore, S.P. Sander, D.M. Golden, R.F. Hampson, M.J. Kurylo, C.J. Howard, A.R. Ravishankara, C.E. Kolb, M.J. Molina, Chemical Kinetics and Photochemical Data for Use in Stratospheric Moleling, JPL Publication 97-4, JPL, Pasadena, 1997.
[3] D.J. Lary, J. Geophys. Res. 101 (1996) 1505.
[4] Y.L. Yung, J.P. Pinto, R.T. Watson, S.P. Sander, J. Atmos. Sci. 37 (1980) 339.
[5] S. Solomon, M. Mills, L.E. Heidt, W.H. Pollock, A.F. Tuck, J. Geophys. Res. 97 (1992) 825.

[6] J.B. Renard, F. Lefevre, M. Pirre, C. Robert, D. Huguenin, Comptes Rendus de l Academie des Sciences Serie II Fascicule A – Sciences de la Terre et des Planetes 325 (1997) 921.
[7] J.B. Renard, M. Pirre, C. Robert, D. Huguenin, J. Geophys. Res. 103 (1998) 25383.
[8] M. Larichev, F. Maguin, G. Le Bras, A. Mellouki, G. Poulet, Chem. Phys. Lett. 172 (1990) 430.
[9] D.R. Hanson, A.R. Ravishankara, Geophys. Res. Lett. 22 (1995) 385.
[10] O.V. Rattigan, D.J. Lary, R.L. Jones, R.A. Cox, J. Geophys. Res. 101 (1996) 23021.
[11] J. Kölm, A. Engdahl, O. Schrems, B.A. Nelander, Chem. Phys. 214 (1997) 313.
[12] D.E. Tevault, N. Walker, R.R. Smardzewski, W.B. Fox, J. Phys. Chem. 82 (1978) 2733.
[13] C. Miller, S.L. Nickolaisen, J.S. Francisco, S.P. Sander, J. Chem. Phys. 107 (1997) 2300.
[14] H.S.P. Müller, C.E. Miller, E.A. Cohen, Angew. Chem. Int. Ed. Engl. 35 (1996) 2129.
[15] J. Kölm, O. Schrems, P. Beichert, J. Phys. Chem. A 102 (1998) 1083.
[16] H.S.P. Müller, E.A. Cohen, J. Chem. Phys. 106 (1997) 8344.
[17] Z. Li, J. Phys. Chem. A 103 (1999) 1207.
[18] R. Lide, CRC Handbook of Chemistry and Physics, 78th ed., CRC Press, Barton Ridge, 1997, pp. 4–46.
[19] T.J. Lee, J. Phys. Chem. 99 (1995) 15074.
[20] H.S.P. Müller, E.A. Cohen, J. Chem. Phys. 106 (1997) 8344.
[21] W. Levason, J.S. Ogden, J. Turner, J. Am. Chem. Soc. 82 (1978) 2733.
[22] S.D. Allen, M. Poliakoff, J.J. Turner, J. Mol. Struct. 157 (1987) 1.
[23] G. Herzberg, Molecular Spectra and Molecular Structure II, Krieger, Malabar, FL, 1988 (chapter 2).
[24] H.S.P. Müller, H. Willner, J. Phys. Chem. 97 (1993) 10589.
[25] J. Ortigoso, R. Escribano, J.B. Burkholder, C.J. Howard, V.J. Lafferty, J. Mol. Spectrosc. 95 (1982) 157.
[26] G. Maier, A. Bothur, Z. Anorg. Allg. Chem. 612 (1995) 743.
[27] G. Herzberg, Molecular Spectra and Molecular Structure I, Van Nostrand, New York, 1950, p. 534.
[28] Z. Li, J.S. Francisco, J. Chem. Phys. 111 (1999) 5780.
[29] S. Guha, J.S. Francisco, Chem. Phys. 247 (1999) 387.
[30] S. Guha, J.S. Francisco, J. Phys. Chem. A 102 (1998) 2072.
[31] P.A. Thiel, T.E. Madey, Surf. Sci. Rept. 7 (1987) 211.
[32] R.I. Masel, Principles of Adsorption and Reaction on Solid Surfaces, Wiley, New York, 1996, pp.133–142.
[33] L. Chu, L.T. Chu, J. Phys. Chem. A. 103 (1999) 8640.